Austin Chemical Engineering

Open Access

Austin Publishing Group

Review Article

Use of Automation to Link Aspen HYSYS with Third-Party Software for Simulating Complex Chemical Engineering Problems

Valverde JL[1]; Giroir-Fendler A[2]; Ramírez A[3]; Ferro VR[4*]

[1]Facultad de Ciencias y Tecnologías Químicas, University of Castilla La Mancha, Avda, Spain

[2]Univ. Lyon, Université Claude Bernard Lyon 1, CNRS, IRCELYON, France

[3]Dr. Antonio Ramirez, CNETE (National Center in Environmental Technology and Electrochemistry), Canada

[4]Department of Chemical Engineering, Universidad Autónoma de Madrid, Spain

***Corresponding author: Valverde JL**

Facultad de Ciencias y Tecnologías Químicas, University of Castilla La Mancha, Avda. Camilo José Cela 12, 13071, Ciudad Real, Spain.

Tel: +34 926 29 53 00

Email: joseluis.valverde@uclm.es

Received: September 13, 2023

Accepted: October 10, 2023

Published: October 17, 2023

Abstract

Automation of process simulators with third-party software allows programmers to expose objects within a program to be used by other applications, access the parameters of a simulation, and estimate physical properties. This paper presents six typical examples of automation for process simulation by linking Aspen HYSYS with MS Excel VBA: determination of the existence and composition of homogeneous azeotropes, optimisation of a distillation tower with side draws, evaluation of the relative gain array of a process, determination of the temperature and concentration profiles inside a catalyst particle by considering the reaction and simultaneous non-isothermal internal and external diffusion phenomena, a solution to a multistage separation problem and the simulation of the thermal cracking of ethane with coke formation.

Keywords: Automation; Aspen HYSYS; MS Excel VBA; Programming; Complex processes

Introduction

Chemical process engineers deal with two types of tasks [23]: the design of new processes and the analysis of existing ones for modifying or optimising them. Currently, these activities are strongly rely on computational modelling and simulation of the processes. The simulation of complex processes requires numerous equations. These equations are related, among other things, to the fundamentals of the process operations involved, the mass and energy balances of each individual operation and the overall process, the phase and chemical equilibria (based on the activity coefficient or equations of state models), the kinetics of heat and mass transport and chemical reactions, and equipment sizing. Additionally, models for manipulating information within process simulations are required: for instance, for algorithms to ensure convergence when recycling information. Many of these equations can be differentiated entirely and even partially. Both the convergence and accuracy of the simulation results strongly depend on the suitability of the models (including property models) and the algorithms employed to solve the equation systems. However, several models and algorithms are complex and difficult to implement or program.

Commercial process simulators, such as Aspen Plus, Aspen HYSYS, Unisim, VMGSim, ProMax, and ChemCad, are very robust program packages capable of solving complex tasks related to all the issues typical of process engineering and offer chemical engineers the opportunity to make fast and complex calculations.

Aspen HYSYS is a process simulator widely used at the industrial level, particularly for conceptual design, control, optimisation, and process monitoring at different stages of any project. A clear advantage of this simulator if compared with its counterpart Aspen Plus is that its architecture permits the integration of the steady-state and dynamic models in a single unit. The competence of process simulators can be improved by interesting developments, such as the integrated analysis methodology developed by Aspen Technology and implemented in the Aspen ONE program suite [4]. This allows access to economic, energetic, and safety analyses of the process and equipment design directly from the Aspen Plus and Aspen HYSYS process simulators.

Citation: Valverde JL, Giroir-Fendler A, Ramírez A, Ferro VR. Use of Automation to Link Aspen HYSYS with Third-Party Software for Simulating Complex Chemical Engineering Problems. Austin Chem Eng. 2023; 10(3): 1105.

In commercial process simulators, all questions related to the models, selection, and computational implementation have received significant attention and have been properly addressed. Moreover, commercial process simulators contain large databases of the physical properties of pure components and mixtures, as well as models for the calculation of thermodynamic and other physical and transport properties. For example, the Property Method in Aspen Plus or a Fluid Package in Aspen HYSYS comprises a phase equilibrium model and different models for physical property calculations. Rigorous property estimation is essential for guaranteeing accurate results in process simulations [12,18,28]. However, the availability of process simulators in this field does not exempt users from the responsibility to select a property method or fluid package that provides a sufficiently accurate representation of the system under consideration. Different models must often be checked against measured data to select the most accurate model. Occasionally, a tedious search is required to collect the parameters of the selected model, or it may be necessary to adjust some model parameters to achieve a better description of the measured data. All these issues require considerable computational effort if automatic realisation is desired.

Despite the advantages that simulators provide to process engineers, several restrictions related to their use can be identified. First, to make an effective use of the simulators, process engineers must know the guidelines and assumptions of the models provided by each simulator [20]: each program has its own specific "rules" of procedure, language, and/or capabilities. Thus, it is important to understand the cases in which they are useful, and how to extract information from them. Moreover, it is difficult to evaluate certain properties or algorithms used by a specific simulator because they can neither provide satisfactory solutions nor converge. However, the more robust and complex a process simulator becomes, the farther it is from the specific and quotidian needs of a common user. The appearance and consolidation of enterprises and process engineering consulting, such as Process Ecology (http://processecology.com) and Billington Process Technology AS (http://bpt.no), which aim to develop user models and apps for use with a specific process simulator, describe this phenomenon well. They expand capabilities by adding new "resources" to the existing process simulators.

A solution to these issues is to automate the simulation process with third-party software such as MS Excel VBA. Automation is described by the Aspen Technology, Inc. company as the use of third party tools such as Visual Basic to programmatically run a simulator as Aspen HYSYS. Using this functionality, the complexity of a simulation can be hidden by building a front end in another program created by the user, which allows access to only the important parameters of the simulation. Automation allows programmers to expose objects within a program for use in other applications. Using an automation client, such as Visual Basic for Applications (VBA), embedded inside MS Excel, the end user can write code to access these objects and interact with Aspen HYSYS. The end user does not need to see the Aspen HYSYS source code or understand what is required to expose the objects. Using the Visual Basic code, it is possible to send and receive information to and from HYSYS, respectively. The exposed objects enable performing nearly any action through the Aspen HYSYS graphical user interface. In this manner, end users can introduce algorithms for solving specific problems that are not considered by simulators and take advantage of their extraordinary capability to estimate physical properties. There are numerous possibilities and the potential for innovative solutions is endless. Another factor to consider is that automation saves time and reduces the probability of error from tedious manual calculations.

Some examples of automation can be found in literature. Aspen Dynamic and MATLAB Simulink software were used to analyse the sequencing of the distillation columns in the second phase of the South Pars Gas Refinery to separate the feed of normal paraffin into four mixtures of products [27]. A straightforward method for calculating the physical and chemical exergies of a material stream was proposed by linking Aspen HYSYS with the MS Excel VBA code [1]. Computer-aided exergy calculations made the exergy analysis more accessible in the HYSYS process simulator, providing more insight into the nature of the irreversibilities associated with specific processes. Similarly, Aspen HYSYS was used to simulate a depropanizer process by generating input-output data to develop the plant model and conduct performance tests, whereas MATLAB-Simulink was used to conduct model identification, design the model predictive control (MPC), and implement the multivariable control action to reduce the variation in product purity due to operational constraints [47]. VBA tools have also been linked with Aspen HYSYS for safer design of heat exchanger networks [40]. An interface between the commercial software Aspen HYSYS and MS-Excel VBA was used to study the effects of environmental relative humidity on the performance of the natural-gas liquefaction process [43]. Recently, two more studies have demonstrated the capability of automation procedures based on the use of Aspen HYSYS to effectively simulate processes. Thus, a transcritical heat-driven compression refrigeration machine with CO_2 as the working fluid was simultaneously simulated and optimised from thermodynamic and economic viewpoints [31], and an optimisation-simulation strategy was applied by coupling the aforementioned simulator with a programming tool (MATLAB) to produce a precise steady-state simulation-based optimisation of an entire green-field saturated gas plant [3].

MS Excel VBA was also linked with Aspen Plus to simulate a hybrid pervaporation–distillation process [50]. The Gensym G2 and Aspen HYSYS process simulators were used to introduce a knowledge-based simulation-optimisation framework to generate sustainable alternatives to the HAD process [22]. The hierarchical design method implemented by these authors as a decision support system was used to generate alternative designs, sustainability metrics, and multi-objective optimisation. VMGSim and MS Excel VBA were used to control the loop configuration and eco-efficiency of the chemical processes [39]. In this manner, the properties of all material and energy streams of a simulated case were extracted and processed using MS Excel VBA, and exergy computations were performed.

In recent years, the digitalisation of the chemical industry has attracted the attention of specialists with different profiles [38]. To create digital twins of physical assets, process simulators are embedded into (more complex) central models, where different programming languages and applications are used [9]. To achieve this, process simulators should be linked to other programs; that is, automation and extensibility should play an important role. The concept of central model is related to that of Model Based Systems Engineering (MBSE). MBSE approaches are a vital part of digital threads (defined as graphs whose nodes are elements in various enterprise repositories, tools, and version control systems). Commercial software as Syndeia™, which is built on various open standards, open-sources projects, and

libraries, etc., enables engineering teams to develop and manage a digital thread for any complex system by connecting models and data from diverse modelling and simulation tools, enterprise applications, and data repositories collaboratively and concurrently. Correspondingly, the digitalisation of the industrial chemical sector has become a definitive stimulus for both the theoretical and practical development of process simulator automation.

The authors of this paper have reported several studies related to the use of Aspen HYSYS and Aspen Plus to simulate different chemical processes. Thus, the gasification of animal waste was simulated in a dual gasifier using Aspen Plus [13], and in an integrated process (pine gasification, syngas cleaning, and methanol synthesis) using Aspen Plus [42]. Finally, the COSMOSAC property model was used in Aspen Plus to study CO_2 absorption [10] and liquid-liquid separation of aromatic-aliphatic mixtures [11,29] with ionic liquids as solvents. Most recently, the binary interaction parameters of the e-NRTL model for 171 salts in water were obtained and validated using the compiled data of mean ionic activity coefficients vs. molality [48]. The e-NRTL equation was solved with Aspen Plus by linking the process simulator and Excel VBA code via automation as third-party software.

This paper presents six examples of automation for the simulation of processes by linking Aspen HYSYS with third-party software such as MS Excel VBA: determination of the existence and composition of homogeneous azeotropes, optimisation of a distillation tower with side draws, evaluation of the relative gain array of a process, determination of the temperature and concentration profiles inside a catalyst particle by considering the reaction and simultaneous non-isothermal internal and external diffusion phenomena, solution to a multistage separation problem and the simulation of the thermal cracking of ethane with coke deposition. The selected examples correspond to well-known complex engineering problems which have been solved by other authors using different calculation procedures.

The determination of the existence and composition of homogenous azeotropes, analysis of the internal and external diffusion phenomena in heterogeneous catalysis, evaluation of the relative gain array of a process, and simulation of thermal cracking of ethane with coke deposition are examples of computational problems that cannot be solved in Aspen HYSYS. However, these are important questions to resolve in the conceptual and basic design of most processes whose solution forces the use of other external programs, unlike Aspen HYSYS, if this is used as the main simulator in engineering calculations. This procedure entails an undesired transfer of information between different programs, which can consume considerable time or be a source of severe errors.

However, although Aspen HYSYS has several algorithms for solving optimisation tasks, it may not have a straightforward solution within this program, depending on the nature of the problem raised. The original configuration of the optimiser, which is recommended for general optimisation problems, may fail when searching for the optimal conditions independent of the selected scheme. The remaining configurations implemented in the Aspen HYSYS optimiser require the support of the Derivative Utility, whose definition is complex.

Regarding the fifth case selected in this study to illustrate the advantages of Aspen HYSYS automation with MS Excel VBA, it is important to recognise that the program allows the simulation and design of multistage operations in a versatile and powerful manner using a rigorous Distillation Column model. However, column convergence may be difficult if the model is not accurately specified. This issue is frequent in the first stages of the conceptual design of separation operations when insufficient information, both in quantity and quality, is available for specifying the calculation. In these cases, shortcut models are strongly recommended because they may produce reasonably good designs if used properly [5,6,51]. In Aspen HYSYS the Shortcut Column model based on the Fenske–Underwood–Gilliland approximations is available and allows for good oriented designs. However, the Shortcut column model cannot display significant information on the column design, such as the column profiles of temperature and composition.

Finally, in the last case, the simulation of the thermal cracking of ethane with coke deposition cannot be simulated because the formation of coke cannot be introduced, which could also affect the open diameter of the plug flow reactor where this process is performed without resorting to extensibility procedures.

In summary, the main contribution of the current study is to demonstrate that the connexion of Aspen HYSYS with a third party software allows to compute complex processes and operations by using advanced algorithms, which are not implemented in the commercial simulator.

Computational Details

Aspen HYSYS V11 was used as the reference simulator in this study. Converged Process Flow Diagrams (PFD) were defined for each example. Process variables such as the molar flow rates, pressure, temperature, and molar enthalpy used in the different computations were imported or exported from Aspen HYSYS to MS Excel VBA and vice versa via Object Linking and Embedded (OLE) automation. The VBA codes controlled the process and performed all external computations using Aspen HYSYS.

Figure 1 shows the VBA code used in Case 6 for connecting Aspen HYSYS and defining the objects used to send and extract information to and from the different streams, respectively (Figure 2). In a previous work, more information about the way to make the automation process is described [49].

Results and Discussions

Case 1: Determination of the Existence and Composition of Homogeneous Azeotropes

Determining the existence and composition of homogeneous azeotropes is important from both theoretical and practical perspectives [33,34,35]. The strict determination of azeotropes from experiments alone is expensive. Computational prediction of azeotropes is a method for reducing this cost because the computational results can be used to narrow the experimental search space.

Assuming ideal vapour behaviour and a Poynting correction factors of one, the following expression can be derived.

$$y_i P = x_i \gamma_i^L P_i^{sat}, \quad i \in C, \qquad [1]$$

Where C is the set of components, P is the system pressure; γ_i^L is the activity coefficient of component i in the liquid phase; P_i^{sat} is the vapour pressure of component i; y_i and x_i are the mole fraction of component i in the vapour and liquid phases, respectively. Using the homogeneous azeotropic condition

$x_i = y_i$, $i \in C$, C nonlinear equations can be defined:

$$F(i) = (x_i - y_i)^2 = 0, \quad i \in C \qquad [2]$$

All possible solutions yield the composition of the existing azeotropes. The solution of this set of equations can also predict the boiling points of the C pure components because this situation $x_i = y_i$ is also satisfied. Both solutions are called *Singular Points*. In this study, the Levenberg–Marquardt algorithm for solving systems of nonlinear equations was used [36]. This algorithm, which was initially derived by the author to evaluate parameters by regression in nonlinear models, was effectively extended to solve systems of nonlinear equations. This algorithm has been used and implemented as an MS Excel VBA tool in several previous studies [2,8,19,21,30,48].

In this study, the presence of azeotropes in a liquid ternary mixture of acetone, chloroform, and methanol at 1 atm was analysed. As mentioned in Introduction, Aspen HYSYS has no tool that allows the estimation of azeotropes, unlike Aspen Plus. Case 1 utilised the advantage of automation for evaluating azeotropes using Aspen HYSYS.

The Aspen HYSYS process flow diagram used in this study is shown in Figure 1. UNIQUAC was used as a Fluid Package. As Aspen HYSYS cannot modify the molar fraction of a stream, three streams of pure acetone, chloroform, and methanol were created. Thus, the composition of the stream *Feed* was defined as the sum of the three pure streams. MS Excel VBA sends the molar flow values for each stream proportional to x_i. These streams were mixed to obtain the stream *Feed*. This stream was conditioned with a heater (*Heat Exch*) to obtain a new one, *To Sep*, with a vapour fraction of 0, which corresponded to the boiling temperature of the mixtures, and was in turn returned to the MS Excel VBA application. The latter stream is applied to a separator (*Separator*). The composition of the stream *Vapour*, which corresponded to y_i, was also returned to the MS Excel VBA code.

Because different solutions can be found, and they are presumably dependent on the initial values considered in the iterative procedure, the strategy followed here is coincidental to that reported elsewhere based on interval mathematics [33], which considers a sequence of intervals, that is, the initial upper and lower bounds on all variables. Since the optimization procedure used starts to compute solutions from a set of initial values of the unknowns, an algorithm was implemented to discard solutions equal to those previously computed. Solutions with numerical values of the function

$$S = \sum_{i=1}^{C} (x_i - y_i)^2 \qquad [3]$$

Higher than 10^{-12} were automatically rejected.

The results are listed in Table 1, along with those estimated by Aspen Plus considering UNIQUAC-Ideal as the Property Method, and those experimentally obtained and reported elsewhere [25] at the same pressure. Some discrepancies, especially relevant to the prediction of the ternary azeotrope, were found when the experimental results and those predicted with Aspen HYSYS-Excel VBA were compared.

Case 2: Optimization of a Distillation Tower with Side Draws

This case is taken from Seider et al. [45]. The distillation tower requires optimisation. A feed containing normal paraffins from n-C_5 to n-C_9 was fed to the 25 stages tower (including the condenser and reboiler) at Stage 15 and counted upward from

Table 1: Solutions obtained in Case 1: comparison with experimental data and those estimated by Aspen Plus. Singular points of the ternary mixture: acetone-chloroform-methanol.

Aspen HYSYS-EXCEL-VBA							
Iterations	**2**	**2**	**2**	**22**	**23**	**22**	**19**
S (eq.3)	$<10^{-50}$	$<10^{-50}$	$<10^{-50}$	10^{-33}	10^{-24}	10^{-23}	10^{-15}
T (ºC)	56.06	61.10	64.48	55.36	53.70	60.04	63.81
$x_{acetone}$	1.000	0.000	0.000	0.759	0.000	0.276	0.388
$x_{chloroform}$	0.000	1.000	0.000	0.000	0.655	0.169	0.612
$x_{methanol}$	0.000	0.000	1.000	0.241	0.345	0.555	0.000
Aspen Plus							
T (ºC)	56.14	61.10	64.54	55.24	54.09	67.46	64.61
$x_{acetone}$	1.000	0.000	0.000	0.777	0.000	0.311	0.341
$x_{chloroform}$	0.000	1.000	0.000	0.000	0.673	0.252	0.659
$x_{methanol}$	0.000	0.000	1.000	0.223	0.327	0.437	0.000
Experimental data [25]							
T (ºC)	56.80	61.21	64.55	55.24	53.33	57.67	64.47
$x_{acetone}$	1.000	0.000	0.000	0.775	0.000	0.381	0.363
$x_{chloroform}$	0.000	1.000	0.000	0.000	0.650	0.241	0.637
$x_{methanol}$	0.000	0.000	1.000	0.225	0.350	0.378	0.000

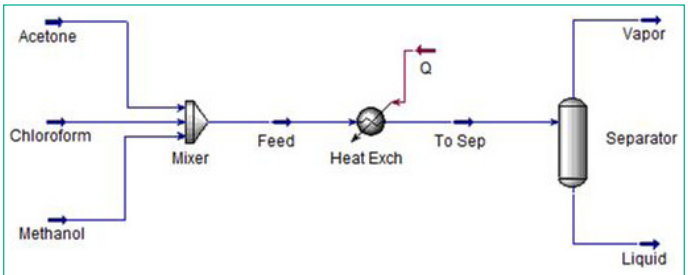

Figure 1: Aspen HYSYS process flow diagram used in Case 1.

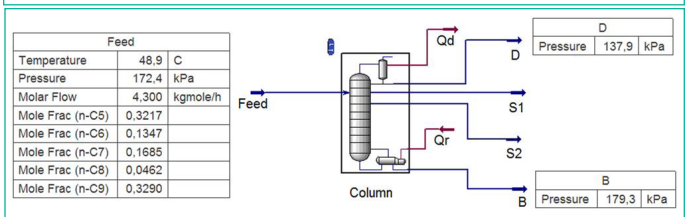

Figure 2: Aspen HYSYS process flow diagram used in Case 2.

the partial-reboiler stage. The objective is to adjust the operating conditions to achieve a distillate (D) concentrated in n-C_5, a side draw at stage 20 ($S1$) concentrated in n-C_6, a second side draw at stage 10 ($S2$) concentrated in n-C_7 and n-C_8, and a bottom product (B) concentrated in n-C_9. The operating conditions to be adjusted were the reflux ratio and flow rates of the distillate and two side draws. The optimisation problem to be solved is as follows:

$$\text{Maximize} \quad Function = D_{C5} + S1_{C6} + S2_{C7} + S2_{C8} + B_{C9} \qquad [4]$$

$$\text{w.r.t.} \quad R, D, S1, S2$$

$$\text{s.t.} \quad 5 \le R \le 10$$

$$0.1 \le D/F \le 0.7$$

$$0.1 \le S1/F \le 0.7$$

$$0.1 \le S2/F \le 0.7$$

$$(D + S1 + S2)/F \le 0.95,$$

where R is the reflux ratio; F, D, $S1$, $S2$ and B are the molar flow rates of the feed, distillate, two side draws, and bottom product streams, respectively; and the subscript denotes the molar flow rate of a specific chemical species in that stream.

In this study, the Compass Search algorithm was used [7],

which was implemented using an MS Excel VBA tool. The Aspen HYSYS process flow diagram used in this study is shown in Figure 2. The Peng–Robinson software was used as the Fluid Package. Different variables were sent, extracted, and returned to Aspen HYSYS.

Results are listed in Table 2 along with those estimated by the optimization tool integrated in Aspen HYSYS and those reported by Seider et al. [45] by considering ideal behaviour of both liquid and vapour phases. Although the objective function computed for the three situations were similar in value, differences were observed among the prediction made by Seider et al. [45], most likely owing to the Fluid Package considered, and that obtained with the other two procedures.

Case 3: Evaluation of the Relative Gain Array of a Process

The Relative Gain Array (RGA) is used for find best pairing that corresponds to good controller performance a widely used method for determining the best input-output pairings for multivariable process control systems to minimise the number of interactions among the resulting loops [17] (Chen and Seborg, 2002). The steady-state gain that is used in pairing analysis purpose is obtained from closed and open loop simulation of the process.

If a process with two outputs (y_1 and y_2) and two inputs (m_1 and m_2) is considered, by assuming that the manipulated variable m_2 remains constant, a step change in the input manipulated variable m_1 of magnitude Δm_1 can cause a change, Δy_1 and Δy_2, from the previous steady state of output variables y_1 and y_2, respectively. The open-loop static gain between y_1 and m_1 when m_2 is kept constant is given by.

$$\left(\frac{\Delta y_1}{\Delta m_1}\right)_{m_2} \quad [5]$$

Thus, the open loop gain matrix (A) can be derived:

$$A = \begin{pmatrix} \left(\frac{\Delta y_1}{\Delta m_1}\right)_{m_2} & \left(\frac{\Delta y_1}{\Delta m_2}\right)_{m_1} \\ \left(\frac{\Delta y_2}{\Delta m_1}\right)_{m_2} & \left(\frac{\Delta y_2}{\Delta m_2}\right)_{m_1} \end{pmatrix} \quad [6]$$

The RGA, Λ, can be computed using two simple operations, which avoids evaluating closed-loop gains:

$$Z = (A^{-1})^T, \quad [7]$$

$$\Lambda = A^{\circ}Z \text{ . (dot or Hadamard product of A and Z)} \quad [8]$$

Each element of the dot product is, in turn, each element of the matrix Λ is the product.

$$\lambda_{ij} = a_{ij} * a_{ij} \quad [9]$$

Each row and column of matrix Λ sums to 1. The relative gain is a useful measure of interaction. In this manner, the control loops are selected by pairing the controlled outputs y_i with the manipulated variables m_j in such a way that the relative gains, λ_{ij}, are positive and as close as possible to unity.

The case presented in Figure 3 was considered as an example. Three variables require control: level of liquid and pressure in the *Separator* and temperature of the stream *Liquid*, with three other manipulated variables, flow rate of the stream *Liquid* (valve), flow rate of the stream *Vapour,* and heat duty in *Cooler* represented by stream *Q*. In the steady-state simulations performed using Aspen HYSYS, the liquid level in the tank could not be modified. In addition, it is common to control the level of liquid in a tank with a valve inserted into the liquid effluent from this vessel (stream *Liquid*). Thus, only two manipulated variables (flow rate of stream *Vapour* and heat duty in *Cooler*

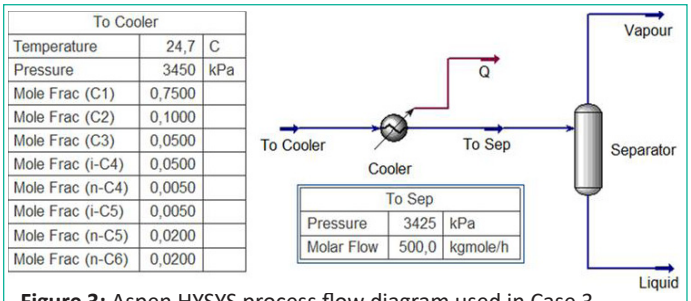

Figure 3: Aspen HYSYS process flow diagram used in Case 3.

represented by stream *Q*) and two controlled variables (pressure in the *Separator* and temperature of the stream *Liquid*) were considered. Both open-loop gain matrix (A) and relative gain array (Λ) were evaluated using MS Excel VBA. One manipulated variable was slightly modified (0.1% of its value), while keeping the other variable constant. This modification affected the controlled variables, which allowed the computation of the open-loop static gains.

Table 3 presents the results of the study. Thus, two controllers should be defined by pairing the variable temperature of *Liquid* with the heat duty in *Cooler* and the variable pressure in *Separator* with the flow rate of *Vapour* (valve).

Case 4: Determination of the Temperature and Concentration Profiles inside a Catalyst Particle

On the pore walls of a solid catalyst, chemical reactions occur simultaneously with diffusion, indicating that these two processes are not strictly consecutive and must be considered simultaneously. Thus, the steady-state mass and heat balances for an arbitrary reaction using spherical geometry are [15]:

$$\frac{1}{r^2}\frac{d}{dr}\left(r^2 D_{eA}\frac{dC_{As}}{dr}\right) - r_s[C_{As}, T_s]\rho_s = 0, \quad [10]$$

$$\frac{1}{r^2}\frac{d}{dr}\left(r^2 \lambda_e \frac{dT_s}{dr}\right) + (-\Delta H) r_s[C_{As}, T_s]\rho_s = 0, \quad [11]$$

where r is radial position in a spherical particle; C_{As} is the molar concentration of reactant A inside the particle; D_{eA} is the effective diffusivity of reactant A; T_s is the temperature inside the particle; r_s is the reaction rate as a function of C_{As} and T_s; ρ_s is the density of the catalyst; $_e$ is the effective thermal conductivity in the solid particle; and *(-ΔH)* is the heat of reaction.

If external temperature and concentrations gradients are considered, the boundary conditions are

$$r = 0: \quad \frac{dC_{As}}{dr} = 0 \quad \therefore \quad \frac{dT_s}{dr} = 0, \quad [12]$$

$$r = R: \quad D_{eA}\frac{dC_{As}}{dr} = k_g(C_A - C_{As}^s) \quad \therefore \quad \lambda_e \frac{dT_s}{dr} = h_f(T - T_s^s), \quad [13]$$

where R is the radius of the particle; C_A is the molar concentration of Reactant A in the bulk fluid; T is the temperature of the bulk fluid; C_A^s is the molar concentration of Reactant A at the surface of the solid; T_s^s is the temperature at the surface of the solid; k_g is the mass transfer coefficient from the bulk fluid to the solid interface; and h_f is the heat transfer coefficient of the film surrounding the particle. By solving these equations, the concentration of Reactant A and the temperature profiles inside the particle can be determined using the following two effectiveness factors:

$$\eta = \frac{\text{rate of reaction with pore diffusion resistance}}{\text{rate of reaction at surface conditions}}, \quad [14]$$

$$\eta_B = \frac{\text{rate of reaction with pore diffusion resistance}}{\text{rate of reaction at bulk fluid conditions}}, \quad [15]$$

The heat transfer correlation, h_f, relating the Nusselt number to the Prandtl and Reynolds numbers for a flow around a sphere is [14,44]:

Table 2: Solutions obtained in Case 2: comparison with results obtained by optimization tool integrated in Aspen HYSYS and those reported by Seider et al. by considering ideal behaviour of both liquid and vapor phases [45].

	Aspen HYSYS-MS Excel-VBA	Aspen HYSYS (Optimization Tool)	Seider et al.
Function (kmol/h)	3.874	3.869	3.828
D (kmol/h)	1.377	1.365	1.520
R	10.000	9.885	10.000
S1 (kmol/h)	0.580	0.602	0.454
S2(kmol/h)	1.036	1.005	0.980

Table 3: Relative gain array in Case 3.

	Controlled variables	
Manipulated variables	T_{Liquid} (ºC)	Sep Pressure (kPa)
Q duty (kJ/s)	0.99682288	0.003177122
Vapour Flow rate (kmol/s)	0.00317712	0.996822878

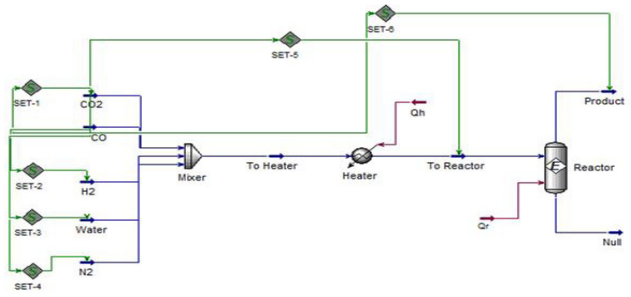

Figure 4: Aspen HYSYS process flow diagram used in Case 4.

$$Nu = 2 + 0.6Re^{1/2}Pr^{1/3} \;\therefore\; \left(\frac{h_f d_p}{\lambda}\right) = 2 + 0.6\left(\frac{u\rho d_p}{\mu}\right)^{1/2}\left(\frac{\mu c_p}{\lambda}\right)^{1/3}, \quad [16]$$

where d_p is the diameter of the particle; u, λ, ρ, μ, and C_p are the free-stream velocity, thermal conductivity, fluid density, viscosity, and specific heat of the fluid under bulk conditions, respectively.

k_g can be computed using the Frossling correlation [16]:

$$Sh = 2 + 0.6Re^{1/2}Sc^{1/3} \;\therefore\; \left(\frac{k_g d_p}{D_{Am}}\right) = 2 + 0.6\left(\frac{u\rho d_p}{\mu}\right)^{1/2}\left(\frac{\mu}{\rho D_{Am}}\right)^{1/3}, \quad [17]$$

where D_{Am} is the molecular diffusivity of A in the multicomponent mixture. The binary diffusion coefficients, D_{ij}, can be computed using the semi-empirical Fuller–Schettler–Giddings relation [17]:

$$D_{ij} = \frac{10^{-7}T^{1.75}\left(\frac{1}{M_1}+\frac{1}{M_2}\right)^{1/2}}{P\left[\left(\sum_i v_{i1}\right)^{1/3}+\left(\sum_i v_{i2}\right)^{1/3}\right]^2}\left(\frac{m^2}{s}\right) \quad [18]$$

where T is the temperature (K); M_i is the molecular weight (g/mol); and V_{ij} are the volumes of the parts of molecule j [17].

By considering an arbitrary reaction:

$$aA + bB + \cdots \leftrightarrow rR + sS + \cdots \quad [19]$$

the molecular diffusivity of A in a multicomponent mixture can be computed as follows [15]:

$$\frac{1}{D_{Am}} = \frac{1}{1+\delta_A y_A}\sum_{k\neq j}^{N}\left\{\frac{1}{D_{Ak}}\left(y_k + y_j\frac{\alpha_k}{|\alpha_A|}\right)\right\}, \quad [20]$$

where y_j is the molar fraction of species j; α_j is the stoichiometric coefficient of species j in Equation [18]; N is the number of components in the multicomponent mixture; and.

$$\delta_A = \frac{(r+s\ldots)-(a+b+\cdots)}{a}, \quad [21]$$

Finally, it is possible to find an estimation of D_{eA} through D_{Am} [15]:

$$D_{eA} = D_{Am}\frac{\varepsilon^{1.5}}{2.46} \quad [22]$$

where ε is the particle porosity.

Evidently, D_{eA} must not be considered a constant. Thus, Equations [10] and [11] can be written as follows:

$$\frac{1}{r^2}\left(2rD_{eA}\frac{dC_{As}}{dr} + r^2\left[\left(\frac{dD_{eA}}{dC_{As}}\right)_{T_s}\frac{dC_{As}}{dr} + \left(\frac{dD_{eA}}{dT_s}\right)_{C_{As}}\frac{dT_s}{dr}\right]\frac{dC_{As}}{dr} + r^2D_{eA}\frac{d^2C_{As}}{dr^2}\right) - r_s[C_{As}, T_s]\rho_s = 0 \quad [23]$$

$$\frac{1}{r^2}\left(2r\lambda_e\frac{dT_s}{dr} + r^2\lambda_e\frac{d^2T_s}{dr^2}\right) + (-\Delta H)r_s[C_{As}, T_s]\rho_s = 0 \quad [24]$$

The terms $\left(\frac{dD_{eA}}{dC_{As}}\right)_{T_s}$ and $\left(\frac{dD_{eA}}{dT_s}\right)_{C_{As}}$ can be evaluated numerically.

In addition to the difficulty in solving the model, the critical point is to evaluate the physical properties: λ, , μ, C_p, and ($-\Delta H$). Aspen HYSYS was used for this purpose.

In this case, the Water–Gas Shift (WGS) was considered.

$$CO + H_2O \leftrightarrow CO_2 + H_2 \quad [25]$$

This exothermic reaction was used to evaluate the temperature and concentration profiles of the solid catalysts. In a previous study [8], the kinetic model of this reaction over a commercial CoMo catalyst was evaluated.

$$r = k_0 exp\left[-\frac{E_a}{RT}\right]\left(\frac{P_{CO}P_{H2O}}{P_{H2}} - \frac{P_{CO2}}{K_P}\right), \quad [26]$$

$$K_P = exp\left(\frac{2073}{T} - 2.029\right), \quad [27]$$

where P_i is expressed in bar and T in K.

In this study, a feed consisting of CO, H_2O, H_2, and N_2 was allowed to flow across a particle of the catalyst located in the centre of a tube. The aim of this case study was to evaluate the concentration of CO and temperature profiles inside the particle. The parameters used in this case are listed in Table 4.

The Aspen HYSYS process flow diagram used in this study is shown in Figure 4. The Peng–Robinson software was used as

Table 4: Parameters used in Case 4. WGS reaction over a commercial CoMo catalyst [8].

Physical properties of the catalyst		**Feed conditions**	
ρ_s (kg/m³)	1150	P (bar)	19
λ_e (W/m.K)	0.4	T (ºC)	500
ε	0.429	Flow rate (Ndm³/s)	10
Geometrical factors		**Feed composition (molar fraction)**	
d_p (m)	0.01	CO	0.1573
Tube diameter (m)	0.1	CO_2	0
Kinetic parameters		H_2	0.0571
k_0 (mol/bar.kg.s)	452.6	H_2O	0.7395
E_a/R (K)	10187.6	N_2	0.0461

Table 5: Some physical properties derived from the data transfer from Aspen HYSYS to the MS Excel-VBA tool apart from the effectiveness factor defined by equations [14] and [15].

Physical properties of the fluid			
D_{eA} (m²/s)	8.6988E-07	**Re**	8032.7
m (kg/m.s)	2.5395E-05	**Pr**	0.697
r (kg/m³)	5.704	**Sc**	5.118
C_p (J/kg.K)	1954.7	**Sh**	94.674
l (W/m.K)	0.0712	**Nu**	49.683
G(kg/m².s)	20.399	**k_g (m/s)**	0.0082
		h_f (W/m².K)	353.743
Effectiveness factors			
η	0.2170		
η_B	0.2167		

the Fluid Package. Five input streams (CO_2, CO, H_2, water, and N_2) were used to define the composition of the input mixture automatically, as discussed above. MS Excel VBA sent the molar flow values for each stream proportional to the molar fractions considered.

These streams were mixed to obtain stream *To Heater*, which was affected by the mixing heat. This stream was then conditioned with a heater (*Heater*) to compensate for the heat and obtain a new stream, *To Reactor*. The temperatures of the feed and latter streams were fixed at those of stream CO. The physical properties: λ, ρ, μ, and C_p were extracted from the latter stream. The heat of the reaction was computed from the energy stream *Qr* as follows:

$$(-\Delta H) = -\left[\frac{Qr\ Duty}{flowrate\ of\ CO\ in\ stream\ To\ Reactor - flowrate\ of\ CO\ in\ stream\ Product}\right] \quad [27]$$

Equations [23] and [24], along with their corresponding boundary conditions, were solved using a finite-difference procedure which was applied to the spatial dimension. Twenty interior points and the boundary conditions were used to reduce the problem to a system of 44 nonlinear equations which were solved using the Levenberg–Marquardt algorithm [36]. The concentration of CO and the temperature profiles inside the particles are shown in Figure 5. Table 5 lists some physical properties derived from the data transfer from Aspen HYSYS to the MS Excel VBA tool, apart from the effectiveness factors defined in Equations [14] and [15]. These results clearly show the importance of the external and internal limitations of the heat and mass transfer phenomena in a catalytic process, which in turn affect the effectiveness factor values, which are significantly lower than one.

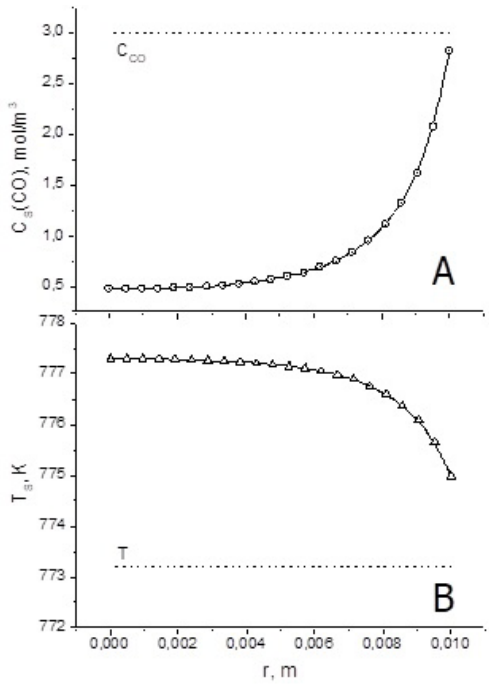

Figure 5: Case 4. Concentration of CO (A) and temperature (B) profiles inside the particle.

Table 6: Parameters used in Case 6. Simulation of thermal cracking of ethane with coke deposition.

Geometry and physical properties		Operating conditions	
d_t (m)	0.108	m_{ethane} (kg/s)	0.5-5
Tube thickness (m)	0.008	Steam dilution (kg/kg)	0.51
k_{coke} (W/m.K)	6.46	p_{inlet} (bar)	2.9
k_{wall} (W/m.K)	-8.432 + 3.04 10^{-2} T(K)	T_{inlet} (ºC))	650
□$_c$ (kg/m^3)	1600	T_{outlet} (ºC)	830

Case 5: Solution of Multistage Separation Problems

Luyben, based on another previous study [26], proposed an alternative design for the butyl acetate process [32]. One of the simulated columns, named in the original paper as *C2*, was adopted in this case. A binary mixture of methyl acetate and methanol was added to the column. This binary system formed an azeotrope with a methyl acetate close to 0.65 (molar fraction). The simulation data for Aspen HYSYS are shown in Figure 6. UNIQUAC-PR was selected as the Fluid Package.

In this study, a simulation procedure based on the McCabe–Thiele method [37,45] was proposed because, as observed in the rigorous Aspen HYSYS simulation, the molar flows of the vapour and liquids exiting from consecutive stages in the rectifying and stripping sections were constant, particularly in the former.

The Aspen HYSYS process flow diagram used in this study is shown in Figure 7. Pure-component streams of acetate and methanol were introduced to define the composition of the feed mixture automatically. Furthermore, two parallel circuits were considered. First, the vapour fraction and pressure of the stream *Feed* were determined before being expanded to the conditions existing in the column. The resulting stream (*Col In*) was transferred to a separator (*Separator 2*). The molar flows of the exiting streams were used to evaluate the mass balance at the feed stage. On the contrary, the other circuit was used to evaluate the temperature of a stage and the composition of the liquid exiting from it in equilibrium with the vapour conducted to the next stage. For this purpose, the vapour fraction and pressure of stream *To Sep 1* were fixed.

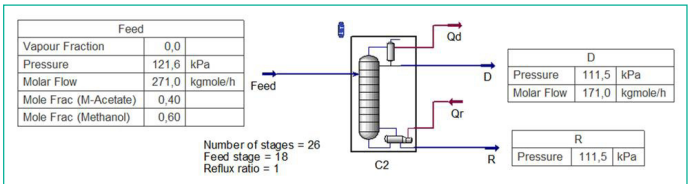

Figure 6: Aspen HYSYS process flow diagram of the example adapted from (Luyben, 2011).

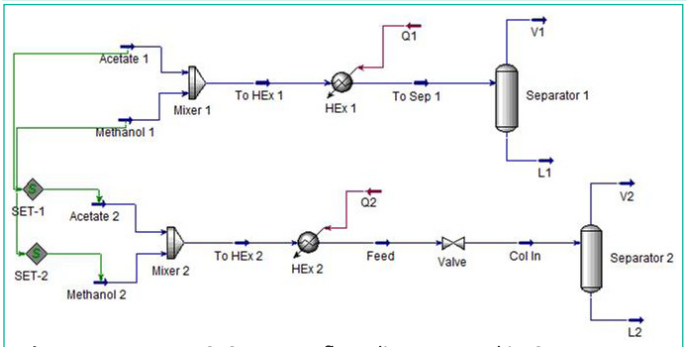

Figure 7: Aspen HYSYS process flow diagram used in Case 5.

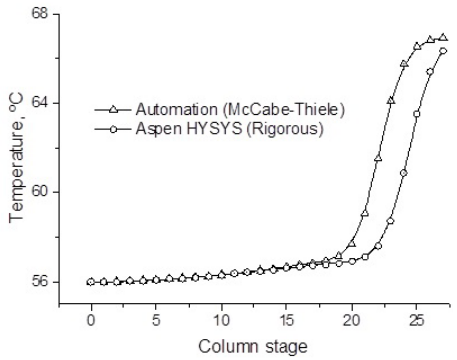

Figure 8: Temperature profiles computed in the column considered in Case 5.

Similar values for the composition of methyl acetate and methanol in the bottom and distillate and the flux of heat removed and supplied to the column were computed using both the methods. The heat removed and supplied (condenser and reboiler duties) to the column computed using Aspen HYSYS were 1.098 10^7 and 1.100 10^7 kJ/h, respectively, whereas those computed using the automation process were 1.095 10^7 and 1.000 10^7 kJ/h, respectively. Finally, Figure 8 compares the temperature profile inside the column, computed using Aspen HYSYS, with the automated process. In the figure, Stages 0 and 27 correspond to the condenser and reboiler, respectively. These differences can be attributed to the assumptions considered in the McCabe–Thiele method, which allows the heat balance in each stage to be discarded. The temperature profiles computed for this column are similar to those reported by Luyben [32].

Case 6: Simulation of the Thermal Cracking of Ethane with Coke Deposition

The production of ethylene, a basic feedstock in the petrochemical industry, by the thermal cracking of ethane is one of the most crucial processes in the chemical industry. This process has been well analysed by Prof. Froment and his group [15,24,41,46]. Cracking was performed in long coils suspended vertically in large gas-fired furnaces. If the conversion is too low, the product distribution may not meet the specifications; if it is too high, the presence of secondary reactions leads to coke formation by the accumulation of 0.01-m thick layers, causing an increase in the pressure drop of the fluid circulating inside the reactor and hindering the heat transfer process. This situation is challenging to account for in the simulator because it does not allow the dynamic inclusion of a increasing amount of coke without creating an extremely complex code (extensibility). In this example, the following reactions are considered.

$$C_2H_6 \rightarrow C_2H_4 + H_2 \;\therefore\; r_1 = 4.65\ 10^{13} exp\left[-\frac{273200}{RT}\right] C_{C_2H_6} \quad [28]$$

$$C_2H_4 + H_2 \rightarrow C_2H_6 \;\therefore\; r_2 = 9.98\ 10^{8} exp\left[-\frac{136870}{RT}\right] C_{C_2H_4} C_{H_2} \quad [29]$$

$$2C_2H_6 \rightarrow C_3H_8 + CH_4 \;\therefore\; r_3 = 3.85\ 10^{11} exp\left[-\frac{273190}{RT}\right] C_{C_2H_6} \quad [30]$$

$$C_3H_6 \rightarrow C_2H_2 + CH_4 \;\therefore\; r_4 = 9.81\ 10^{8} exp\left[-\frac{154580}{RT}\right] C_{C_3H_6} \quad [31]$$

$$C_2H_2 + CH_4 \rightarrow C_3H_6 \;\therefore\; r_5 = 6.06\ 10^{4} exp\left[-\frac{29480}{RT}\right] C_{C_2H_2} C_{CH_4} \quad [32]$$

$$C_2H_2 + C_2H_4 \rightarrow C_4H_6 \;\therefore\; r_6 = 1.03\ 10^{12} exp\left[-\frac{172750}{RT}\right] C_{C_2H_2} C_{C_2H_4} \quad [33]$$

$$C_2H_4 + C_2H_6 \rightarrow C_3H_6 + CH_4 \;\therefore\; r_7 = 7.08\ 10^{13} exp\left[-\frac{253010}{RT}\right] C_{C_2H_4} C_{C_2H_6} \quad [34]$$

$$C_2H_6 \rightarrow 2C + 3H_2 \;\therefore\; r_8 = 5.00\ 10^{11} exp\left[-\frac{2240000}{RT}\right] C_{C_2H_6}^{1.34} \quad [35]$$

$$C_3H_6 \rightarrow 3C + 3H_2 \;\therefore\; r_9 = 2.77\ 10^{6} exp\left[-\frac{116000}{RT}\right] C_{C_3H_6}^{2.89} \quad [36]$$

$$C_4H_6 \rightarrow 4C + 3H_2 \;\therefore\; r_{10} = 5.61\ 10^{15} exp\left[-\frac{274000}{RT}\right] C_{C_4H_6}^{2.17} \quad [37]$$

where R=8.314 kJ/kmol. K, C_i, r_j (j=1–7) and r_j (j=8–10) are expressed in kmol/m, kmol/ m.s, and g_{coque}/ m^2.s, respectively.

The continuity equations, assuming a straight tube, can be written as follows (Plehiers, P. M., Reyniers, G. C., Froment, G. F., Simulation of the Run Length of an Ethane Cracking Furnace, Ind. Eng. Chem. Res. 1990, 29, 636-641):

$$Mass: \frac{dF_j}{dz} = -\left(\sum n_{ij}\, r_i\right)\frac{\pi d_t^2}{4}, \quad [38]$$

$$Energy: \frac{dT}{dz} = \frac{1}{\sum F_j c_{pj}}\left[Q(z)\,\pi d_t + \frac{\pi d_t^2}{4}\sum r_i\,(-\Delta H)_i\right], \quad [39]$$

$$Momentum: \frac{dp_t}{dz} = \frac{\frac{d}{dz}\left(\frac{1}{M_m}\right) + \frac{1}{M_m}\left(\frac{1}{Tdz}\frac{dT}{dz} + \frac{0.092\left(\frac{up\,d_t}{\mu}\right)}{d_t}\right)}{\frac{1}{M_m p_t} - \frac{p_t}{aG^2RT}} \quad [40]$$

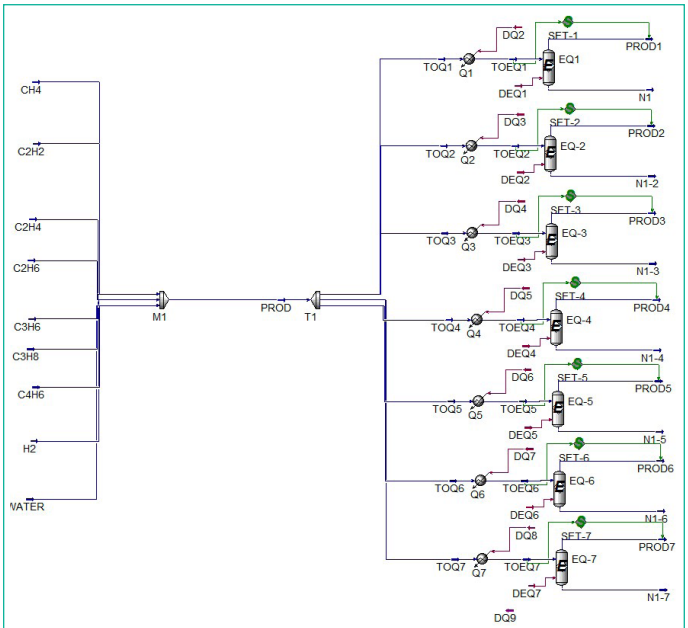

Figure 9: Aspen HYSYS process flow diagram used in Case 6.

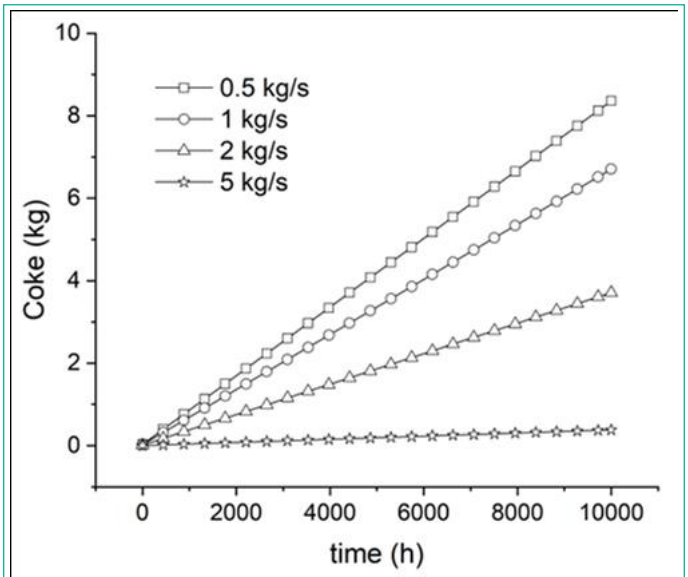

Figure 10: Case 6. Evolution of the coke produced vs. the time on stream.

where c_p is the heat capacity; d_t is the tube diameter; F_j is the molar flow rate of species j; G is the total mass flux; $(DH)_i$ is the heat of reaction i; M_m is the average molecular weight; n_{ij} is the stoichiometric coefficient of species j in reaction i; $_{pt}$ is the total pressure; Q is the heat flux; r is the reaction rate; R is the gas constant; T is the temperature; u is the free-stream velocity; z is the axial coordinate; a is the unit conversion factor; ρ is the fluid density; and μ is the fluid viscosity under bulk conditions.

Coke formation at any time and position is accounted for by the continuity equation:

$$\frac{\partial c_c(z)}{\partial t} = \sum_{i=8}^{10} n_{ic} r_i(z) \;\therefore\; C_c(t=0) = 0, \quad [41]$$

where C_c is the concentration of coke and n_{ic} is the stoichiometric coefficient of coke in reaction i.

In this case, it was assumed that the coke deposition in a particular section was homogeneous. Thus, the thickness of the coke layer (e) can be evaluated at any time using the following equation:

$$\frac{\partial e(z)}{\partial t} = \frac{\sum_{i=8}^{10} n_{ic} r_i(z)}{\rho_c} \;\therefore\; e(t=0\ and\ z=0, L) = 0, \quad [42]$$

where L is the length of the reactor, and r_c is the coke density. The presence of coke affects heat transfer because it adds ad-

ditional resistance which must be considered.

The total amount of coke formed on the inner walls of the plug-flow reactor (m_c) at any time can be computed as follows:

$$m_c(t) = \int_o^L \left[\rho_c \frac{\pi}{4}\left(d_t^2 - \left(d_t - 2e(t)\right)\right)\right] dz. \qquad [43]$$

1. Other model assumptionsThe gas mixture is considered as an ideal gas.

2. Axial dispersions of mass and heat are negligible.

3. Radial concentration gradients are neglected.

4. This case was investigated in a quasi-steady state to simulate the coke deposition rate.

In this study, a feed consisting of C_2H_6, and H_2O were fed into the plug-flow reactor. The aim of this case study was to evaluate the effect of the inlet mass flow on the coke deposition. The parameters used in this case are listed in Table 6.

The Aspen HYSYS process flow diagram used in this study is shown in Figure 9. The Peng–Robinson software was used as the Fluid Package. Nine input streams (CH_4, C_2H_2, C_2H_4, C_2H_6, C_2H_2, C_3H_6, C_3H_8, C_4H_6, H_2, and water) were used to define the composition of the input mixture automatically, as discussed above. MS Excel VBA sent the molar flow values for each stream proportional to the considered molar fractions. These streams were mixed to obtain stream *PROD*, which was affected by the mixing heat. This stream was divided into seven substreams that were conducted with the same number of equilibrium reactors corresponding to each of the seven reactions (Equations [28]–[34]). Temperatures and pressures were defined for the streams entering the different reactors. Specifically, the physical properties, ρ, μ and C_p, were extracted from stream *TOEQ1*. The heat of the reactions was computed from the energy streams *DEQ1* in a similar manner, as defined in Equation [27].

The set of Equations [38]–[40] was solved using the Runge–Kutta fourth order method (100 steps). For coke formation, Equations [41]–[43] were computed according to the Euler method with a step size of 0.04 h and the results were used to correct the rest of the variables by solving the Equations [38]–[40].

Four mass flowrates of ethane were tested: 0.5, 1, 2, and 5 kg/s. The runs were performed for 10000 h. The temperature of the external wall of the tube was set to 830 ºC. Figure 10 shows the evolution of the coke produced versus the time on stream. Despite the coke production, minimal variations in the effluent stream variables (conversion of ethane, temperature, and pressure) were observed. The ethane conversions in the inlet stream were 0.754, 0.687, 0.511, and 0.158 for 0.5, 1, 2, and 5 kg/s of ethane, respectively. The computed outlet pressures were 2.88, 2.84, 2.72, 1.93 bar. These results are consistent with the residence time computed for each run.

Conclusions

This study considered six examples of automation for the simulation of processes by linking Aspen HYSYS with MS Excel VBA: determination of the existence and composition of homogeneous azeotropes (Case 1), optimization of a distillation tower with side draws (Case 2), evaluation of the relative gain array of a process (Case 3), determination of the temperature and concentration profiles inside a catalyst particle by considering the reaction and the simultaneous non-isothermal internal and external diffusion phenomena (Case 4), solution of a multistage separation problem (Case 5), and the simulation of the thermal cracking of ethane with coke deposition (Case 6). Mathematical procedures were followed in the automation process, and Aspen HYSYS simulation flowsheets were extensively adapted in each case.

This manuscript show code about the best way solve complex problems in a reliable way, which are not possible to compute with the simulator itself. Thus, Aspen HYSYS does not implement tools for computing azeotropes (as Aspen Plus does) or evaluating the relative gain array of the process to be used to match manipulated and controlled variables. In addition, this methology allows to extract basic information (physical properties) which could be used to either compute phenomenological models, as that used for evaluate temperature and concentration profiles inside a catalyst particle, or simulate the thermal cracking of ethane with coke deposition, which affects the free section of the tube where the reaction proceeds and impacts on the velocity of the fluid and the pressure drop in the reactor. The latter example is not possible to be implemented in the simulator.

Author Statements

Conflict of Interest

Author Antonio Avalos Ramirez is employed by Centre National en Électrochimie et en Technologies Environnementales Inc. The remaining authors declare that the research was conducted in the absence of any commercial or financial relationships that could be construed as a potential conflict of interest.

References

1. Abdollahi-Demneh F, Moosavian MA, Omidkhah MR, Bahmanyar H. Calculating exergy in flowsheeting simulators: A Hysys implementation. Energy. 2011; 36: 5320-7.
2. Armenise S, García-Bordejé E, Valverde JL, Romeo E, Monzón A. A langmuir-Hinshelwood approach to the kinetic modelling of catalytic ammonia decomposition in an integral reactor. Phys Chem Chem Phys. 2013; 15: 12104-17.
3. Bayoumy SH, El-Marsafy SM, Ahmed TS. Optimization of A saturated gas plant: meticulous simulation-based optimization - A case study. J Adv Res. 2020; 22: 21-33.
4. Beck R. Improving and optimizing conceptual designs: why integrated modeling and economics achieves better processes. An industry white paper. Aspen Publishers Technology, Inc; 2010.
5. Branan C. Rules of thumb for chemical engineers. 4th ed. Burlington: Elsevier, Ma. 2005.
6. Branan CR. Development of Shorcut equipment design methods. In: Asee Annual Conference proceedings. Georgia. Usa: Institute Of Technology. 1985.
7. Davidon WC. Variable metric method for minimization. SIAM J Optim. 1991; 1: 1-17.
8. De La Osa AR, De Lucas A, Romero A, Valverde JL, Sánchez P. Kinetic models discrimination for the high pressure Wgs reaction over A commercial Como catalyst. Int J Hydrog Energy. 2011; 36: 9673-84.
9. De Leeuw V. Creating and deploying digital twins in the process industries. Arc white paper. 2019.
10. De Riva J, Ferro V, Moya C, Stadtherr MA, Brennecke JF, Palomar J. Aspen plus supported analysis of the post-combustion CO2 capture by chemical absorption using the P2228[Cnpyr] And:[66614][Cnpyr]Aha Ionic Liquids. Int J Greenhouse Gas Control. 2018; 78: 94-102.

11. De Riva J, Ferro VR, Moreno D, Diaz I, Palomar J. Aspen plus supported conceptual design of the aromatic–aliphatic separation from low aromatic content naphtha using 4-methyl-N-Butyl-pyridinium tetrafluoroborate ionic liquid. Fuel Process Technol. 2016; 146: 29-38.

12. Economou IG, Kontogeorgis GM, Dohrn R, De Hemptinne J-C. Advances in thermodynamics for chemical process and product design. Chem Eng Res Des. 2014; 92: 2793-4.

13. Fernandez-Lopez M, Pedroche J, Valverde JL, Sanchez-Silva L. Simulation of the gasification of animal wastes in A dual gasifier using aspen plus (R). Energy Convers Manag. 2017; 140: 211-7.

14. Fogler HS. Elements of chemical reaction engineering. 5th ed. Boston: Prentice Hall. 2016.

15. Froment GF, Bischoff KB, De Wilde J. Chemical reactor analysis and design. 3rd. Ed. John Wiley & Sons. Inc. Hoboken. NJ. 2011.

16. Frossling N. Ube die Verdungstung Fallernder Tropfen. Gerlands Beitr Geophys. 1938; 52: 170-216.

17. Fuller EN, Schettler PD, Giddings JC. New method for prediction of binary gas-phase diffusion coefficients. Ind Eng Chem. 1966; 58: 18-27.

18. Gani R, Pistikopoulos EN. Property modelling and simulation for product and process design. Fluid Phase Equilib. 2002; 194-197: 43-59.

19. García E, Rodriguez L, Ferro V, Valverde JL. Prediction of multicomponent ion exchange equilibria by using the E-Nrtl model for computing the activity coefficients in solution. Fluid Phase Equilib. 2019; 498: 132-43.

20. Gil Chaves ID, Guevara Lopez JR, Garcia Zapata JL, Leguizamon Robayo A, Rodriguez Niño G. Process analysis and simulation in chemical engineering. Switzerland: Springer International Publishing. 2016.

21. Gutiérrez-Guerra N, Jiménez-Vázquez M, Serrano-Ruiz JC, Valverde JL, De Lucas-Consuegra A. Electrochemical reforming vs. catalytic reforming of ethanol: A process energy analysis for hydrogen production. Chem Eng Process Process Intensif. 2015; 95: 9-16.

22. Halim I, Srinivasan R. A knowledge-based simulation-optimization framework and system for sustainable process operations. Comput Chem Eng. 2011; 35: 92-105.

23. Haydary J. Chemical process design and simulation. Aspen plus and aspen Hysys applications. Aiche & Wiley. 2019.

24. Heynderickx GJ, Froment GF. Simulation and comparison of the run length of an ethane cracking furnace with reactor tubes of circular and elliptical cross sections. Ind Eng Chem Res. 1998; 37: 914-22.

25. Hiak T, Kurihara K, Kojima K. Vapor-liquid equilibria for acetone plus chloroform plus methanol and constituent binary-system At 101.3 Kpa. J Chem Eng Data. 1994; 39: 714-9.

26. Jiménez L, Costa-López J. The production of butyl acetate and methanol via reactive and extractive distillation. Ii. Process modeling, dynamic simulation, and control strategy. Ind Eng Chem Res. 2002; 41: 6735-44.

27. Khodadoost M, Sadeghi J. Dynamic simulation of distillation sequences in dew pointing unit of south pars gas refinery. J Chem Petrol Eng. 2011; 45: 109-16.

28. Kontogeorgis GM, Folas GK. Thermodynamic models for industrial applications. Wiley. 2010.

29. Larriba M, De Riva J, Navarro P, Moreno D, Delgado-Mellado N, García J, et al. Cosmo-based/aspen plus process simulation of the aromatic extraction from pyrolysis gasoline using the {[4empy] [Ntf2] +[Emim] [Dca]} ionic liquid mixture. Sep Purif Technol. 2018; 190: 211-27.

30. Lazo-Cannata JC, Nieto-Márquez A, Jacoby A, Paredes-Doig AL, Romero A, Sun-Kou MR et al. Adsorption of phenol and nitrophenols by carbon nanospheres: effect of Ph and ionic strength. Sep Purif Technol. 2011; 80: 217-24.

31. Luo J, Morosuk T, Tsatsaronis G, Tashtoush B. Exergetic and economic evaluation of A transcritical heat-driven compression refrigeration system with CO2 as the working fluid under hot climatic conditions. Entropy. 2019; 21: 1164.

32. Luyben WL. Design and control of the butyl acetate process. Ind Eng Chem Res. 2011; 50: 1247-63.

33. Maier RW, Brennecke JF, Stadtherr MA. Computing homogeneous azeotropes using interval analysis. Chem Eng Technol. 1999; 22: 1063-7.

34. Maier RW, Brennecke JF, Stadtherr MA. Reliable computation of reactive azeotropes. Comput Chem Eng. 2000; 24: 1851-8.

35. Maranas CD, Mcdonald CM, Harding ST, Floudas CA. Locating all azeotropes in homogeneous azeotropic systems. Comput Chem Eng. 1996; 20: S413-8.

36. Marquardt DW. An algorithm for least-squares estimation of nonlinear parameters. J Soc Ind Appl Math. 1963; 11: 431-41.

37. Mccabe WL, Thiele EW. Graphical design of fractionating columns. Ind Eng Chem. 1925; 17: 605-11.

38. Morse PM. On the road to digital. Chem Eng, February 2020. 2020: 34-6.

39. Munir MT, Yu W, Young BR. A software algorithm/package for control loop configuration and eco-efficiency. ISA Trans. 2012; 51: 827-33.

40. Pasha M, Zaini D, Mohd Shariff AM. Inherently safer design for heat exchanger network. J Loss Prev Process Ind. 2017; 48: 55-70.

41. Plehiers PM, Reyniers GC, Froment GF. Simulation of the run length of an ethane cracking furnace. Ind Eng Chem Res. 1990; 29: 636-41.

42. Puig-Gamero M, Argudo-Santamaria J, Valverde JL, Sánchez P, Sanchez-Silva L. Three integrated process simulation using aspen plus (R): pine gasification, syngas cleaning and methanol synthesis. Energy Convers Manag. 2018; 177: 416-27.

43. Qyyum MA, Minh LQ, Ali W, Hussain A, Bahadori A, Lee M. Feasibility study of environmental relative humidity through the thermodynamic effects on the performance of natural gas liquefaction process. Appl Therm Eng. 2018; 128: 51-63.

44. Ranz WE, Marshall WR. Evaporation from drops. 1. Chem Eng Prog. 1952; 48: 141-6.

45. Seider WD, Seader JD, Lewin DR, Widagdo S. Product and process design principles. Synthesis, analysis, and evaluation. New York: John Wiley & Sons, Inc; 2009, 3rd. Edition.

46. Sundaram KM, Van Damme PS, Froment GF. Coke deposition in the thermal cracking of ethane. AIChE J. 1981; 27: 946-51.

47. Truong Thanh T, Tufa LD, Mutalib MIA, Abdallah AFM. Control of Depropanizer in dynamic Hysys simulation using Mpc in MATLAB-Simulink. In: Bustam MA, Man Z, Keong LK, Hassankiadeh AA, Fong YY, Ayoub M, Moniruzzaman M, Mandal P, editors Proceeding Of 4th International Conference On Process Engineering And Advanced Materials. 2016.

48. Valverde JL, Ferro VR, Giroir-Fendler A. Estimation of E-Nrtl binary interaction parameters and its impact on the prediction of thermodynamic properties of multicomponent electrolyte systems. Fluid Phase Equilib. 2022; 551: 113264.

49. Valverde JL, Ferro VR, Giroir-Fendler A. Automation in the simulation of processes with aspen Hysys: an academic approach. Comput Appl Eng Educ. 2023; 31: 376-88.

50. Verhoef A, Degrève J, Huybrechs B, Van Veen H, Pex P, Van Der Bruggen B. Simulation of A hybrid pervaporation-distillation process. Comput Chem Eng. 2008; 32: 1135-46.

51. Woods DR. Rules of thumb in engineering practice. Wiley-Vch Verlag, 1st [reprint]. 2008.